



## City Research Online

### City, University of London Institutional Repository

---

**Citation:** Tsavdaridis, K., McKinley, B., Corfar, D. A. & Lawson, R. M. (2024). Cellular Beam End-Posts with Two Connection Types, End Notches and Infill Plates. *Journal of Constructional Steel Research*, 215, 108547. doi: 10.1016/j.jcsr.2024.108547

This is the published version of the paper.

This version of the publication may differ from the final published version.

---

**Permanent repository link:** <https://openaccess.city.ac.uk/id/eprint/32247/>

**Link to published version:** <https://doi.org/10.1016/j.jcsr.2024.108547>

**Copyright:** City Research Online aims to make research outputs of City, University of London available to a wider audience. Copyright and Moral Rights remain with the author(s) and/or copyright holders. URLs from City Research Online may be freely distributed and linked to.

**Reuse:** Copies of full items can be used for personal research or study, educational, or not-for-profit purposes without prior permission or charge. Provided that the authors, title and full bibliographic details are credited, a hyperlink and/or URL is given for the original metadata page and the content is not changed in any way.

---

---

---

City Research Online:

<http://openaccess.city.ac.uk/>

[publications@city.ac.uk](mailto:publications@city.ac.uk)

---



# Cellular beam end-posts with two connection types, end notches and infill plates

Konstantinos Daniel Tsavdaridis<sup>a,\*</sup>, Brett McKinley<sup>b</sup>, Dan-Adrian Corfar<sup>a</sup>, R. Mark Lawson<sup>c</sup>

<sup>a</sup> Department of Engineering, School of Science & Technology, Northampton Square, City, University of London, EC1V 0HB London, UK

<sup>b</sup> University of Central Lancashire, PR1 2HE Preston, UK

<sup>c</sup> The Steel Construction Institute, Silwood Park, SL5 7QN Ascot, UK

## ARTICLE INFO

### Keywords:

Cellular beams  
Infills  
Notches  
Connections  
Vierendeel mechanism  
Tests

## ABSTRACT

A series of 6 shear and bending tests was carried out on end-posts to cellular beams using nominally simply supported end-plate and fin-plate connections in order to determine the shear resistance of the end-posts in comparison with design predictions to EN 1993-1-13. The tests also included end-posts without and with notches to the beam flanges and openings with half infill plates. The cellular beams were 560 mm deep with 400 mm diameter openings.

The test with a narrow end-post connected to a bolted fin-plate failed by in-plane bending of the end-post whereas the same test with an end-plate failed by *Vierendeel* bending at the first opening at 2% higher load. The tests with a narrow end-post and notches to the flanges failed at 86% and 90% of the equivalent test without notches. The test with a half infill plate failed by buckling of the plate at 22 to 26% higher load than the narrow end-post. In all cases, the failure loads were significantly higher than the design predictions using measured properties.

## 1. Introduction

The use of cellular beams with regular circular openings is well established in long span steel and composite construction worldwide, for which a typical example is shown in Fig. 1. The design of cellular beams is also covered by publications, including SCI P355 [6], and AISI Guides [2] and is explicitly covered by a new Part of the forthcoming Eurocode 3 (EN1993-1-13) [4].

Cellular beams are formed by cutting and re-welding rolled steel beams so that the ratio of the opening diameter,  $a_o$ , to finished beam depth,  $h$ , is in the range of  $a_o \geq 0.6 h$  but  $\leq 0.8 h$ . The web slenderness  $d/t_w$  is generally in the range of  $60\epsilon$  to  $80\epsilon$ , where  $d$  is the web depth between the root radii of the rolled section and  $\epsilon = (235/f_y)^{0.5}$  in Eurocode terms.

The modes of failure of cellular beams are pure shear and bending at the centreline of the openings, *Vierendeel* bending due to the transfer of shear across the openings, and web-post shear or buckling for closely spaced openings. Cellular beams used in composite construction can have a heavier bottom Tee than the top Tee for more efficient composite design. Their span-to-depth ratio is generally in the range of 20 to 25 and so limiting the deflections at serviceability often controls the chosen

beam size.

Fabricated (plated) beams may be fabricated from 3 plates and the same rules apply provided that the web slenderness is in the same range as a cellular beam formed from a rolled section.

For the *Vierendeel* failure mode, Redwood [10] proposed that a circular opening may be represented by an equivalent rectangle of length  $0.45a_o$  and depth  $0.9a_o$ , which implies that the critical angle for this local bending resistance of the web-flange Tees is at  $26^\circ$  to the vertical. The equivalent rectangle approach is approximate and generally used in 'hand calculations'.

The 'end-post' is defined as the width of the solid web next to the end connections to the columns or supporting beams. No test results or definitive design guidance exists for the design resistance of the end-posts as affected by the adjacent connections and the possible modes of failure may be different from the adjacent web-posts.

Tsavdaridis and D'Mello [14] performed 7 tests on short span beams with different opening shapes designed to fail in web-post buckling. The angle of the strut and tie was found to be in the range of  $44^\circ$  to  $54^\circ$  to the centre-line of the web opening. These tests showed that the equivalent strut method is more conservative for narrow web-posts compared to the tests and FE modelling. Panedpajaman et al. [9] carried out finite

\* Corresponding author.

E-mail address: [konstantinos.tsavdaridis@city.ac.uk](mailto:konstantinos.tsavdaridis@city.ac.uk) (K.D. Tsavdaridis).

<https://doi.org/10.1016/j.jcsr.2024.108547>

Received 18 December 2023; Received in revised form 9 February 2024; Accepted 11 February 2024

Available online 14 February 2024

0143-974X/© 2024 The Authors. Published by Elsevier Ltd. This is an open access article under the CC BY license (<http://creativecommons.org/licenses/by/4.0/>).

element models of 13 cellular beam tests to investigate and validate their model for web-post buckling. They compared the draft EN1993-1-13 equivalent strut buckling method with 390 simulated FE models and proposed an alternative method with a variable effective length factor depending on the web-post width. Grilo et al. [5] presented 10 tests on 2.66 m span cellular beams subject to a central point load to investigate web-post buckling and they also measured out-of-plane displacements of the web-post on buckling. Moreover, they carried out a parametric study of the tested beams.

A considerable amount of research is available on web-post buckling between circular openings which is likely to be a similar phenomenon to end-post buckling, but there is little information on the modes of failure of end-posts as affected by their connections. The behaviour of moment connections to cellular beams is a subject of great interest in terms of plasticity of the reduced web section (RWS) in seismic design. First numerical studies were conducted on non-composite RWS connections [7,8,15,16] and then composite [11] RWS moment connections with perforated cellular beams. Fully welded and extended end-plate bolted connections were investigated, and the effect of the end-post was considered to understand the stiffness, strength and ductility of such connections under hysteretic loading. Later, Tsavdaridis et al. [13] performed three tests on non-composite connections subject to sagging and hogging moments under cyclic loads. Results indicated that RWS connections can achieve their nominal moment capacity with stable hysteretic cycles without strength degradation. Particularly, they can sustain storey drifts larger than 2% without failing in less ductile modes like tearing of flanges, webs, welds or joint panel zones, fracture of bolts or sudden buckling of end-plates. This good performance derives from the yielding of the critical perforated cross-section and development of *Vierendeel* moments at the edges of the web openings. Tests indicate that

the distance between the first web opening and the column face should be  $<1.5$  times the diameter of the web opening to initiate the mechanism. Almutairi et al. [1] performed tests on four steel-concrete composite connections subject to sagging and hogging moments using beams each with a single large circular web opening next to the connections in which the failure mechanism was by *Vierendeel* bending. The connections were subject to cyclic loading and showed that plasticity in the web flange Tees is a highly ductile failure mode. The end-posts had welded end-plates and the widths of the end-posts were  $0.75 \times$  opening diameter and they did not fail in the tests.

The model for the design of end-posts given in the draft EN-1993-1-13 is an adaptation of the 'strut' buckling model for web-posts between circular openings, which is calibrated against tests. In the draft EN1993-1-13, the minimum width of the end-post for circular openings is given as  $s_e \geq 0.25a_o$ , where  $a_o$  is the opening diameter. If this is not satisfied, an additional infill plate is required in the first opening, which may be in the form of a half infill up to the centreline of the opening or a full infill depending on the load conditions.

Furthermore, many different forms of end connections to cellular beams may be used, which either strengthen or weaken the end-post. Also, beam-to-beam connections often require that notches are cut in the in-coming cellular beam flanges to connect to the supporting beam web. Notches reduce the web depth and concentrate the local stresses in the remaining part of the web between the notches and the openings. Little guidance exists on the limiting dimensions of notches and SCI 'Joints in Steel Construction' [12] gives a maximum notch depth of  $0.1 h$  and a maximum notch length of  $0.2 h$  for solid web beams, where  $h$  is the beam depth and additional checks are required on the lateral stability of the unsupported flange. However, these limiting notch sizes are too large for cellular beams.



(a)



(b)

**Fig. 1.** (a) Cellular beams with infill plate next to the connection in long span composite construction, (b) Un-notched (left) and notched (right) cellular beams “(b) images courtesy of Kloeckner Metals Westok”.

In the absence of test information on the behaviour of end-posts in cellular beams, a series of tests on cellular beam-to-column connections was devised in order to investigate whether the design approach proposed in EN1993-1-13 could be verified and improved. The main aim of the tests conducted in this work was on the failure modes of the end-post and the effect of the connection type rather than the connection itself. The connections to the column flanges were designed as nominally pinned but may have some bending stiffness and resistance. The 6 connection tests included:

- End-plate and fin-plate bolted connections.
- Notched and full depth webs to cellular beams.
- Opening diameters  $a_o \approx 0.7h$ , which is typical of practice for cellular beams.
- End-post widths less than the current limit of  $s_e \geq 0.25 h$ .
- Half web infill plates to the opening to widen the end-post to satisfy the above limit.
- Use of S355 steel in the beams and infill plates.

## 2. Design of End-posts

### 2.1. Design of End-posts to EN1993-1-13

The design method for end-posts presented in the draft version of EN1993-1-13 is based on an adaptation of the web-post strut buckling model that is known to be conservative for large circular openings. This strut action is shown in Fig. 2. The compression force acting on the equivalent strut is taken as equal to the shear force transferred from the top Tee, which is  $N_{ep,Ed} = V_{t,Ed} = 0.5V_{Ed}$  for a symmetric section, where  $V_{Ed}$  is the design shear force.

The effective length of the equivalent strut is taken as the diagonal distance over half of the end-post width and half of the opening depth, as shown in Eq. (1):

$$l_{eff} = [(0.5s_e)^2 + (0.5a_o)^2]^{0.5} = 0.5(s_e^2 + a_o^2)^{0.5} \leq 0.7a_o \quad (1)$$

Where  $a_o$  is the opening depth and  $s_e$  is the end-post width.

The strut slenderness is obtained by dividing the effective length by  $t_w/12^{0.5}$ , which gives an end-post slenderness ratio,  $\bar{\lambda}_{ep}$ , calculated as per eq. (2):

$$\bar{\lambda}_{ep} = 1.75 \frac{(s_e^2 + a_o^2)^{0.5}}{t_w \lambda_1} \leq \frac{2.45 a_o}{t_w \lambda_1} \quad (2)$$

Where  $\lambda_1$  is equal to  $3.14 (E/f_y)^{0.5}$ ,  $t_w$  is the web thickness, and  $f_y$  is the web yield strength.

The buckling resistance of the end-post is obtained from buckling curve 'a' to BS EN1993-1-1 [3], which is justified because the plate restraint to web buckling is greater than that of the web considered as an equivalent strut. The buckling resistance of the end-post is verified using  $\bar{\lambda}_{ep}$  and is given by expression (3):

$$N_{b,i,Rd} = \chi_{ep} b_{eff} t_w f_y \geq N_{ep,Ed} \quad (3)$$

Where  $b_{eff}$  is the effective width of the equivalent strut, equal to  $0.5s_e$  and  $\chi_{ep}$  is the reduction factor due to buckling of the end-post.

For stability of the end-post next to an end-plate connection, the end-post slenderness is reduced by the notional restraint provided by the end-plate according to expression (4):

$$\bar{\lambda}_{ep} \approx 1.75 \frac{((0.7s_e)^2 + a_o^2)^{0.5}}{t_w \lambda_1} \leq \frac{2.1 a_o}{t_w \lambda_1} \quad (4)$$

This equivalent strut method is conservative because it is based on buckling being the limiting mode of failure, whereas it is possible to argue that the transfer of shear by tension in the end-post can increase by a redistribution of shear forces between the Tees.

### 2.2. Design of notched end-posts

Notches to the flanges are often required in beam-to-beam connections. The proposed limiting dimensions of the notches in cellular beams are taken as:

Depth of notch,  $d_n \leq 0.05 h$

Length of notch,  $c_n \leq 0.5s_e$

Where  $h$  is the beam depth.

For stability of the end-post next to a connection with a notch to the compression flange, the end-post slenderness is increased by the partial loss of restraint to the web according to expression (5):

$$\bar{\lambda}_{ep} = 1.75 \frac{((1.2s_e)^2 + a_o^2)^{0.5}}{t_w \lambda_1} \leq \frac{2.7 a_o}{t_w \lambda_1} \quad (5)$$

When verifying the end-post with a notch to the compression flange, the effective width is  $b_{eff} = s_e - c_n$  and  $\leq 0.5s_e$ .

### 2.3. Design for horizontal shear

The end-post horizontal shear force at the centre-line of the opening is given by eq. (6):

$$V_{ep,Ed} = V_{Ed} \frac{(s_e + 0.5a_o)}{h_{eff}} \quad (6)$$

Where  $h_{eff}$  is the vertical distance between the centroid of the Tees.

The limiting horizontal shear resistance of the end-post corresponds to a shear strength of  $0.577 f_y$  to BS EN 1993-1-1 [3].

Although not stated, the horizontal shear resistance of an end-plate connection may be increased by adding a contribution from the end-plate according to eq. (7):

$$V_{ep,Rd} = 0.577 t_w (s_e f_y + t_e f_{y,e}) \quad (7)$$

Where  $t_e$  is the thickness of the end-plate and  $f_{y,e}$  is the yield strength of the end-plate.

For fin-plate connections, it may be assumed that a bolt hole occurs at the centre-line of the opening (as it did in the tests) which gives a horizontal shear resistance as calculated by eq. (8):

$$V_{ep,Rd} = 0.577 t_w (s_e - \Phi) t_w f_y \quad (8)$$

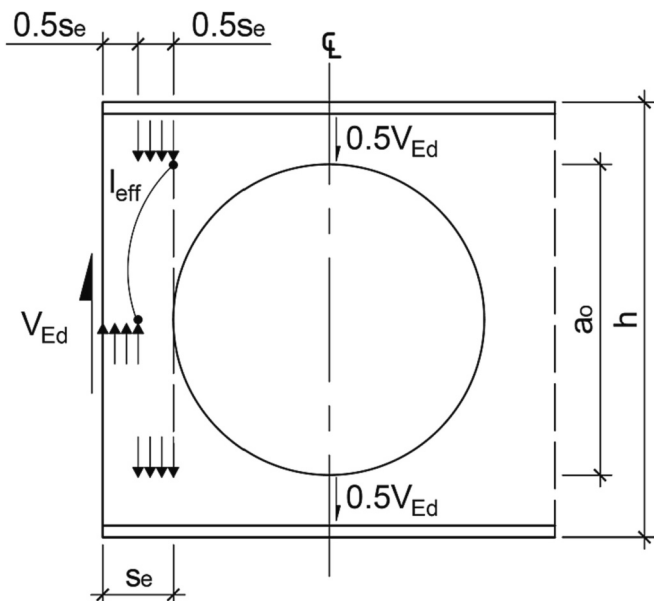


Fig. 2. Illustration of strut buckling model for end-post in EN 1993-1-13.

Where  $\phi$  is the bolt hole diameter.

For narrow end-posts, a further mode of failure is that of in-plane bending of the end-posts due to horizontal shear that is not explicitly covered by EN 1993-1-13. Also, no design methodology is presented for half infill plates to the outer openings. Other modes of failure may occur in moment-resisting connections, which are not covered by this paper.

#### 2.4. Design of half infill plates

A half infill plate acts in compression to transfer the shear force in the top Tee to the full web depth. The following theory may be used to determine the local buckling resistance of the infill plate and the buckling resistance of the end-post with its half infill plate. In this proposed method for half infill plates, the minimum width of the end post is  $s_e \geq 0.5a_o$  and also the length of a notch,  $c_n \leq 0.5s_e$ . If these limits are not satisfied, a full infill plate should be used.

The local stability of the half infill plate is checked first as this may control, and is independent of the end-post. Also, the infill plate may be thinner and of lower yield strength than the parent beam. The local stability of the infill plate is determined for an equivalent strut of width  $b_{eff} = 0.25a_o$  and the effective length is taken as equal to the diagonal distance from the centre of the effective width to mid-height of the plate, as per eq. (9):

$$l_{eff} = 0.5((0.5a_o)^2 + a_o^2)^{0.5} = 0.56a_o \quad (9)$$

The equivalent slenderness ratio of the half infill plate is therefore calculated using eq. (10):

$$\bar{\lambda}_i = \frac{1.95a_o}{t_i \lambda_1} \quad (10)$$

Where  $t_i$  is the thickness of the infill plate ( $\leq t_w$ ) and  $\lambda_1$  is obtained using  $f_{y,i}$ , which is the yield strength of the infill plate.

The buckling resistance of the infill plate is obtained for buckling curve 'a' using  $\bar{\lambda}_i$  as per eq. (11):

$$N_{b,i,Rd} = \chi_i b_{eff} t_i f_{y,i} \quad (11)$$

Where  $b_{eff}$  is the effective width of the half infill plate in compression equal to  $0.25a_o$  and  $\chi_i$  is the reduction factor due to buckling of the infill plate.

For local stability of the infill plate, it is required that  $N_{b,i,Rd} \geq V_{t,Ed} = 0.5 V_{Ed}$  for a symmetric section.

The end-post with its half infill plate is also verified using the design procedure presented in section 2.1 but using the minimum thickness and yield strength of the web and infill plate. It is generally found that the buckling resistance of the end-post with a half infill plate is less than the local buckling resistance of the infill plate, except in the case of a wide end-post or where it is partially stabilised by an end-plate connection.

These design formulae for the end-post shear resistance are used to compare with the end shear force at failure in the tests (see section 4.4).

### 3. Cellular beam tests

Two tests were performed on each of 3 beams with the 2 connection types in order that the effect of the connection-type could be assessed by eliminating the effect of other beam parameters.

The beams were loaded by 2 jacks placed at 803 mm from the ends of the beam and the openings were stiffened by full depth infills and web stiffeners at these points. The beams were 3618 mm long in all tests and were laterally restrained only at mid-span. The columns were 1 m high and their base plates were designed to provide stability to the columns, so that the connections were otherwise not laterally restrained. This was important as the notched beams might fail by lateral movement of the beam flange.

#### 3.1. Details of test beams

The test beams were chosen to be representative of current practice and were designed so that *Vierendeel* bending and vertical shear of the circular openings may both control. The beams were chosen as:

- 406 × 178 × 67 kg/m UB sections (similar to IPE400) cut and re-welded to form a cellular beam of depth  $h = 560$  mm.
- Opening diameter  $a_o = 400$  mm so that  $a_o = 0.71 h$ .
- S355 nominal steel grade.
- Web slenderness,  $d = 75t_w \epsilon$  based on measured properties.

The columns were chosen as 203 × 203 × 60 kg/m UC sections (similar to HEA200). The two generic connection types were chosen as:

- End-plate connections using a 12 mm thick end-plate with 2 × 4 no. M20 bolts to the column flange.
- Fin-plate connection using a 12 mm thick projecting welded plate of 440 mm depth ( $= 0.78 h$ ) with 5 no M20 bolts to the beam web.

The beam details for the tests are shown in Fig. 3. Each beam had a fin-plate connection and an end-plate connection to be able to compare the failure loads of the end-post for the two connection-types directly. The end-plate connection stabilises the end-post to some extent and was expected to give higher failure loads in shear than the fin-plate connection.

The predicted failure shear load for the beam based on *Vierendeel* bending of the opening next to the connection was 250kN using the nominal steel strength. The expected design shear force at the ultimate limit state for an equivalent beam span of 13.5 m (based on span: depth ratio of 24) with a line load of 30kN/m is approximately 200kN.

The nominal and measured dimensions of the test beams are presented in Table 1.

The schematic of the test arrangement is shown in Fig. 4 in which the load points and the supports had to align with the holding down positions in the strong floor. The dimensions of the loading system with the Macalloy bars through the floor slab are shown in Fig. 5.

#### 3.2. Details of end-posts

Three forms of end-post next to the two connection types were devised for the tests:

- Narrow end-post of 90 mm width ( $s_e = 0.225a_o$ ), which is less than the current minimum width ( $s_e = 0.25a_o$ ).
- Narrow end-post with 90 mm wide x 60 mm deep notches to both flanges with a 20 mm radius corner of the notch.
- End-post formed by 200 mm wide half infill plate (actually 203 mm) of 8 mm nominal thickness to create an end-post of width  $s_e = 0.51a_o$ .

The modes of failure that were envisaged and according to the literature are:

- Horizontal shear failure of the narrow end-post at the weld line of the cellular beam.
- End-post bending of the narrow end-post at the first bolt above the centreline.
- Buckling of the web of the end-post at the notch to the flange in the case of a narrow end-post.
- *Vierendeel* bending failure at the first full cell (or half-cell in the case of a half infill).
- Buckling of the half infill plate under the effect of the locally applied shear force from the top Tee.

The shear resistance of the bolted connections themselves was not intended to be the mode of failure, except possibly in the case of the fin-

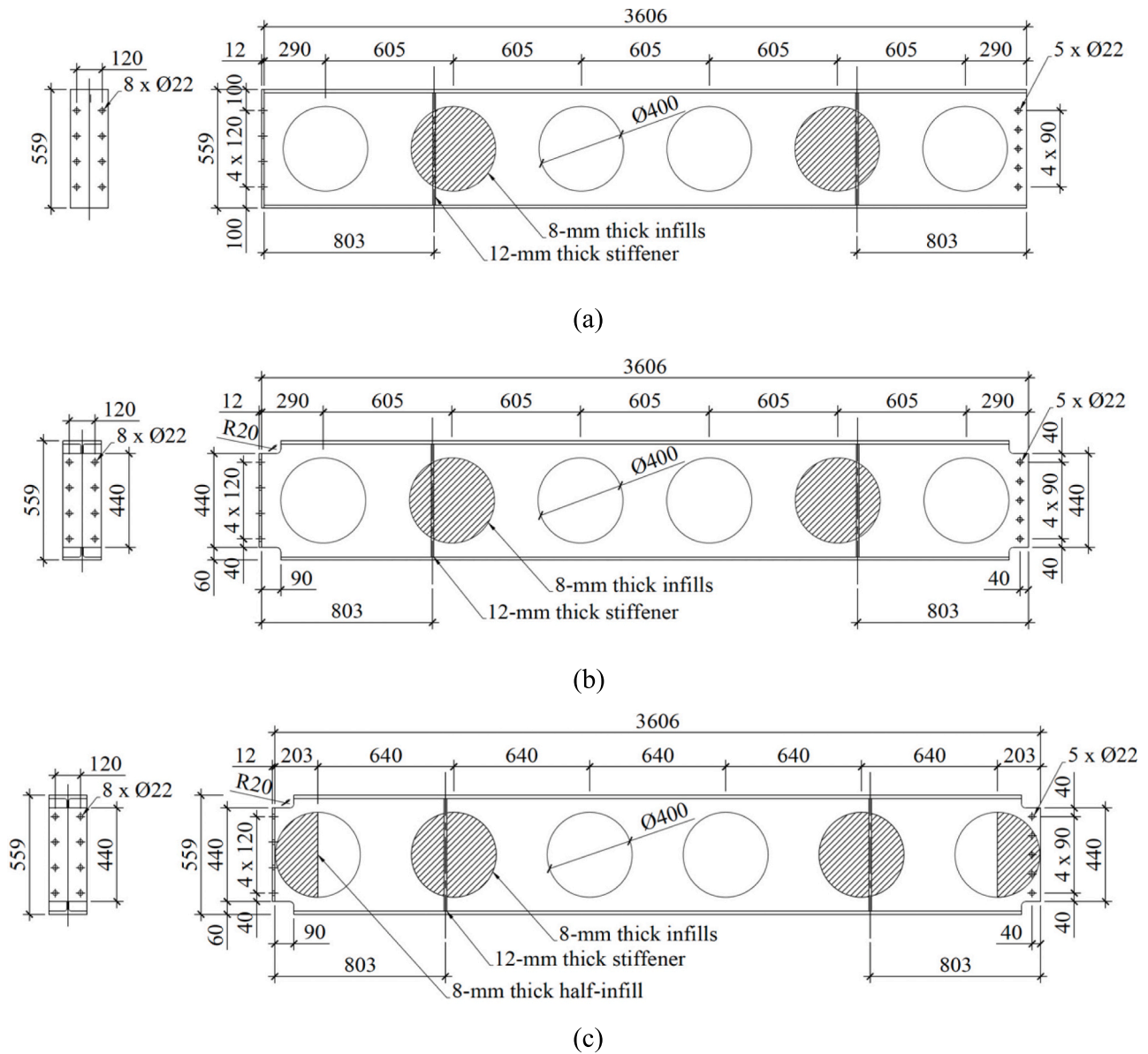


Fig. 3. Details of cellular beams in the tests (each beam having 2 connection types): (a) narrow end-post, (b) narrow end-post with notches, (c) half infill plate end-posts with notches.

Table 1  
Dimensions of the test beams.

Cellular beam properties	Beam depth	Flange width	Web thickness	Flange thickness	Infill plate thickness	Yield strength (beam)	Yield strength (infill plate)
Nominal	560 mm	179 mm	8.8 mm	14.3 mm	8.0 mm	355 N/mm <sup>2</sup>	355 N/mm <sup>2</sup>
Measured	559 mm	179 mm	9.0 mm	14.0 mm	7.8 mm	393 N/mm <sup>2</sup>	469 N/mm <sup>2</sup>

Note: Cellular beams cut and re-welded from 406 × 178 × 67 kg/m UB

plate connection with the half infill, which had a higher predicted failure load. However, of interest to the tests was the effect of the connections on the stability of the end-post and on its horizontal shear resistance as influenced by the bolt holes in the case of a fin-plate and the plate thickness in the case of an end-plate.

### 3.3. Details of instrumentation

The location of the deflection and strain measurements are shown in Fig. 6. The vertical deflections of each test beam were recorded by four

potentiometers, one placed under each of the applied point loads (P01, P04) and another two (P02, P03) closely spaced at the notional mid-span of the specimen. In addition, two horizontal potentiometers (P05, P06) were positioned on the top flange next to the ends of each test beam to measure the in-plane longitudinal displacement between the beam ends and the columns. For the test beams with notches, strain gauges were installed at 45-degree angles on both sides of the web near each of the notched ends in order to be able to determine the onset of yielding there.

Moreover, strain gauges were installed on the columns together with strain gauges at mid-span that allowed the beam bending moment to be

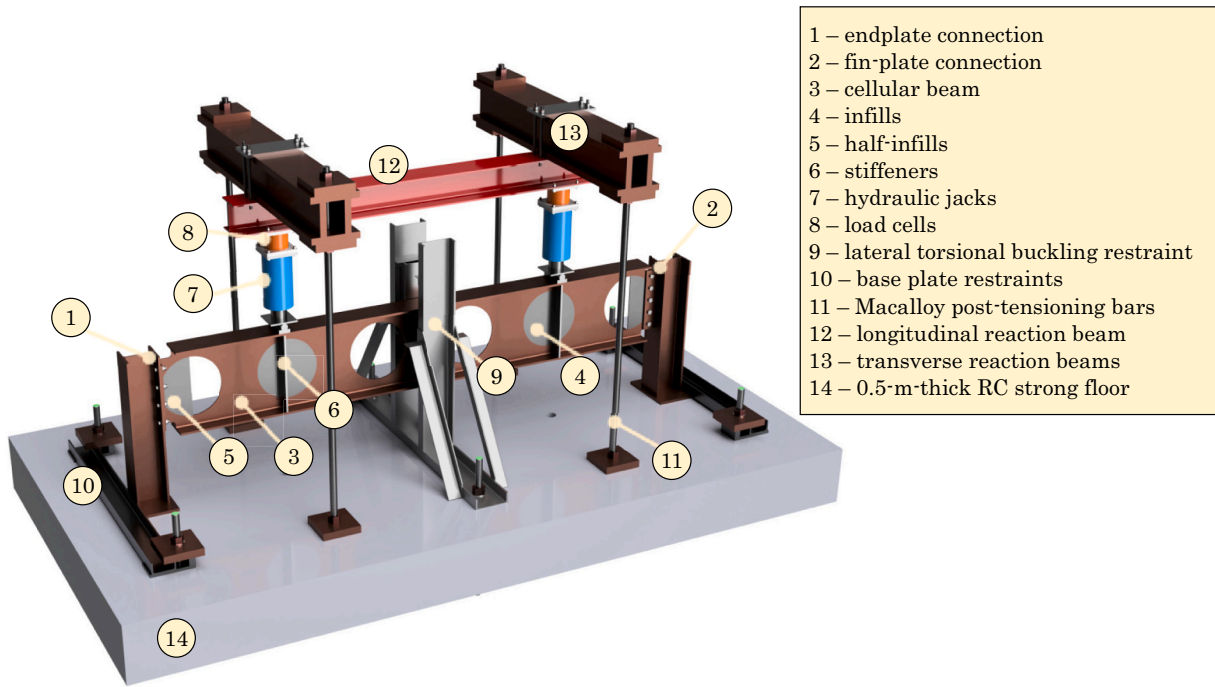
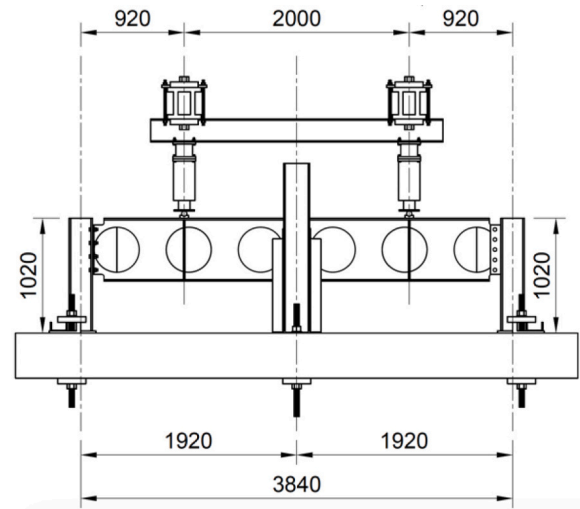


Fig. 4. Schematic of the beam and its loading system.



(a)



(b)

Fig. 5. Test setup: (a) View of the test frame, (b) Dimensions of the loading system and holding down positions.

calculated in relation to the applied moment from the jacks.

### 3.4. Test protocol

After setting-up the test frame, the bolt assemblies were initially left loose and then a small load was applied to the test beam to allow the bearing of all bolts in the bolt holes. This was done to avoid slip in the bolt holes during subsequent test stages.

Two tests were obtained from one beam making 6 tests in total by adopting the following test protocol:

- Load to a jack load of 40kN and un-load to allow for slip of the bolts into bearing.
- Load on both jacks to 200kN as the equivalent factored load on the beam and un-load to 40kN.
- Load on both jacks to failure of one side of the beam firstly in steps of 20kN to 200kN and then in steps of 10kN allowing for 1 min load relaxation on each load increment. Failure occurred on the fin-plate side by the inability to maintain the jack load and the failure mode of the end-post was observed at the associated displacement.
- Unload both jacks to 200kN.
- Increase the load on the jack next to the un-damaged connection (the end-plate side) also in steps of 10kN allowing for 1 min load relaxation. The load on the other jack fell slightly due to the beam displacement. Failure occurred on the end-plate side by the inability to maintain the jack load and the failure mode of the end-post was also observed at the associated displacement.

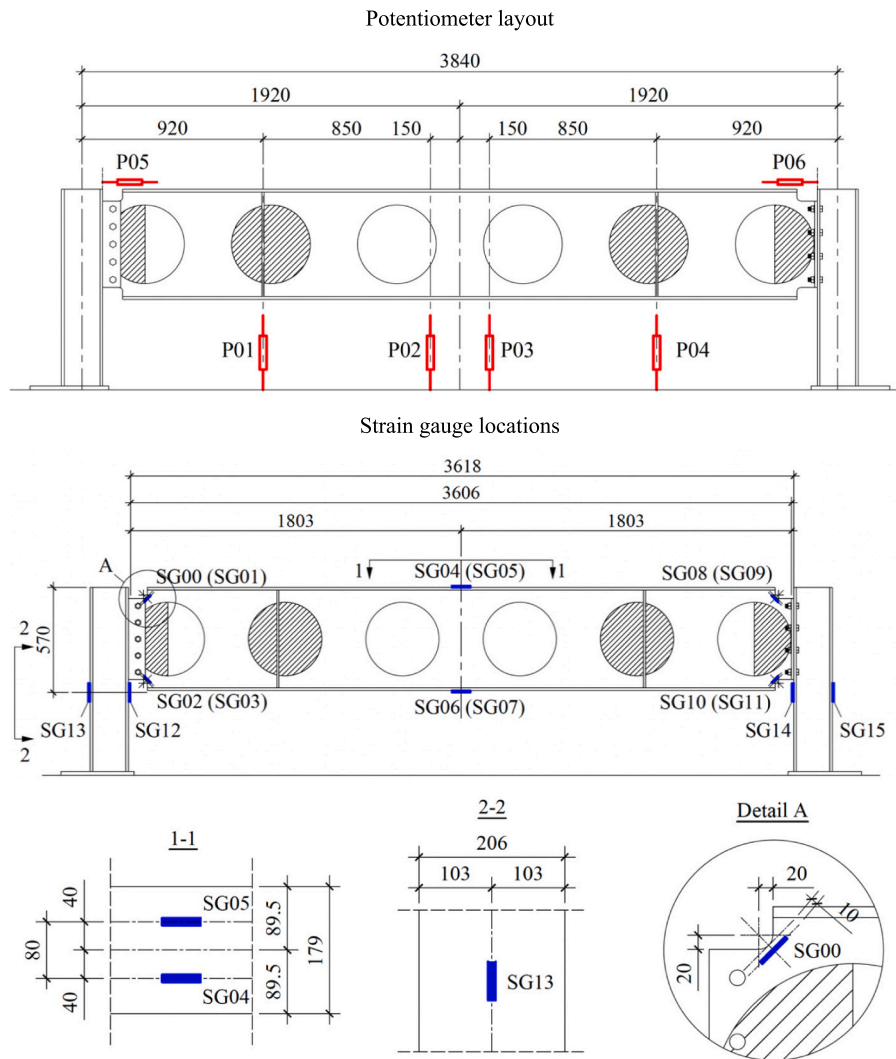


Fig. 6. Instrumentation scheme (shown for test beam with half infill plate end-posts and notches).

- Unload to determine the residual displacement due to deformation of the end-posts.

The shear force on each side of the beam was determined from the beam geometry as shown in expressions (12) and (13):

$$V_1 = \frac{((L - a)P_1 + aP_2)}{L} = 0.78P_1 + 0.22P_2 \tag{12}$$

$$V_2 = \frac{(aP_1 + (L - a)P_2)}{L} = 0.22P_1 + 0.78P_2 \tag{13}$$

Where  $P_1$  and  $P_2$  are the load cell readings for the two jacks,  $a$  is the position of the load point from the adjacent connection equal to 0.803 m,  $L$  is the clear span between the connections equal to 3.618 m, and  $V_1$  and  $V_2$  are the shear forces in the two connections and their end-posts.

The calculated bending resistance of the connections is 56kNm for the full depth end plate and 26kNm for the partial depth end-plate (which are respectively 21% and 10% of the failure moment for test 1 and 3, respectively). The nominal bending resistance of the fin plate connection is 22kNm combined with end-shear (which is 8% of the failure moment for test 1). There may be a difference of 7 to 15kN in the end shear forces due to the bending resistances of the connections, but this effect is relatively small in comparison to the test resistances.

## 4. Results of beam tests

### 4.1. Test on beam with narrow end-post

The beam with a narrow end-post (and without notches) did not satisfy the minimum end-post width and was expected to fail in horizontal shear at the weld-line or by in-plane bending of the end-post. This test is also compared to the equivalent test with notches to the flange.

The load-displacement curve for this test is shown in Fig. 7. The behaviour was linear until a load of about 70% of the shear failure load of 325kN for the fin-plate connection side. Failure occurred by in-plane bending and local buckling of the end-post at the line of the first bolt at 90 mm above the mid-height of the beam as can be seen in Fig. 8a. The in-plane bending is caused by the horizontal shear force in the 90 mm wide end-post, which had reached its yield strength without weld failure.

The test was continued as described in the protocol to a failure load of 331kN on the end-plate side (2% higher than the fin-plate). However, the failure mode on the end-plate side was different in that it occurred by *Vierendeel* bending (Fig. 8b) at the first opening apparently unaffected by the local conditions in the end-post. This is attributed to the strengthening effect of the endplate in in-plane bending in horizontal shear which prevented this mode of failure. The maximum load occurred at a deflection of 21 mm of which about 14 mm was due to plasticity.

The following observations were drawn:

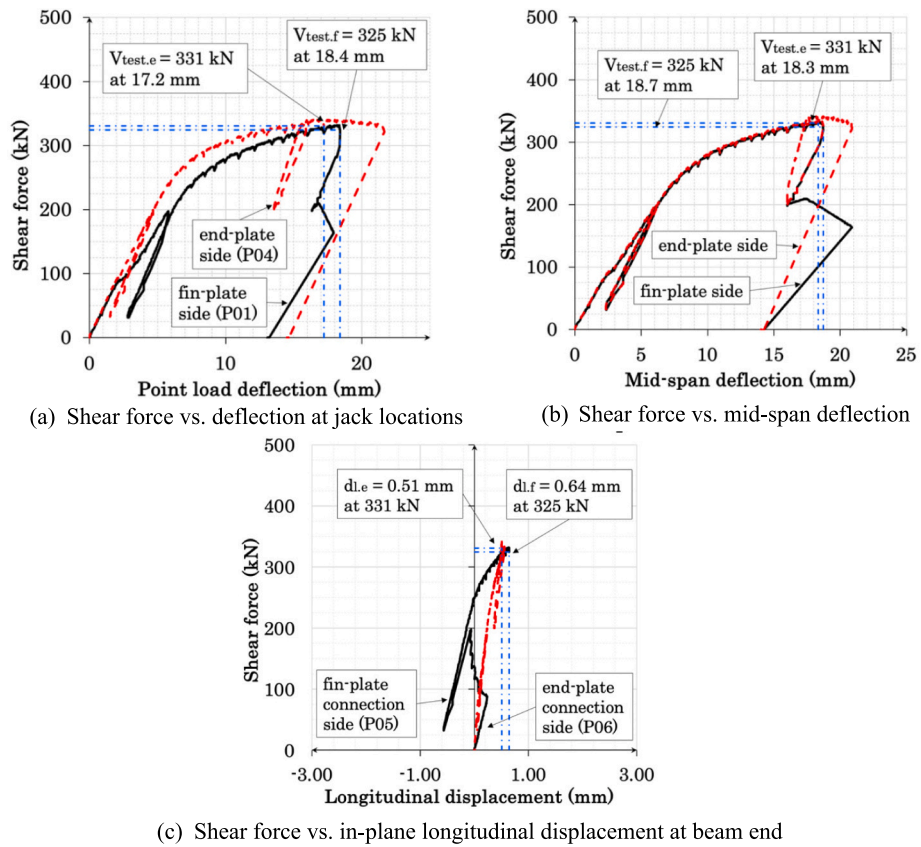


Fig. 7. Load-displacement curves for beam test with narrow end-posts.

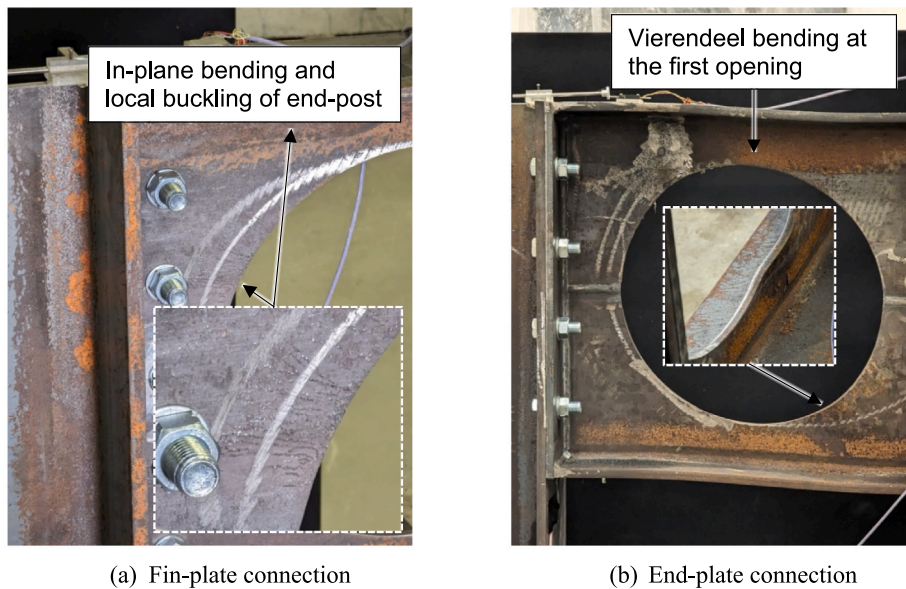
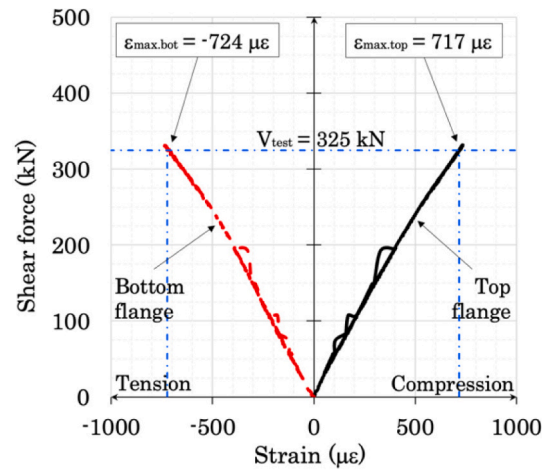
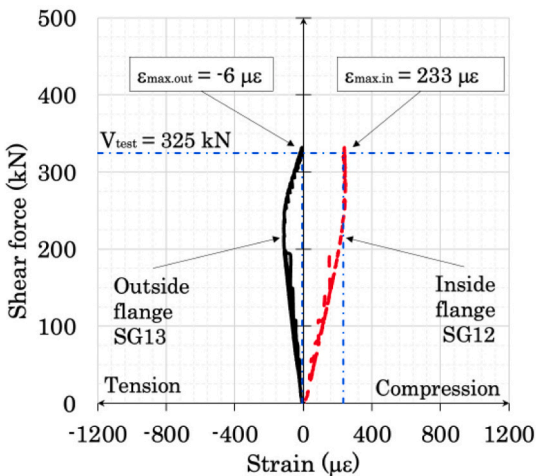


Fig. 8. Failure modes for beam test with narrow end-posts.

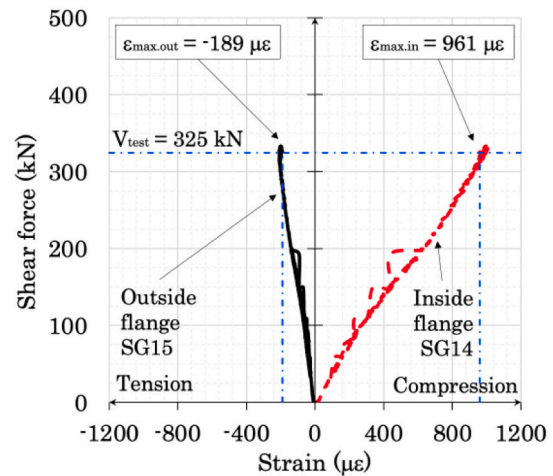
- Fig. 7a shows that the end-plate connection is stiffer than the fin-plate and has some moment resistance.
- Fig. 7c shows that the horizontal displacements are in the range of 0.5 mm for both connections.
- Fig. 8a shows that plasticity occurs next to the second bolt row in the narrow end-post only for the fin-plate connection and not for the end-plate connection.
- Figs. 9b and c show that the high compression strains on the inside flange of the column suggest that the direct shear force from the connection is resisted mostly by the inside flange of the column, while the tensile strains in the outside flanges indicate the presence of hogging moments in the connections.



(a) Beam flanges at mid-span



(b) Column flanges at fin-plate side



(c) Column flanges at end-plate side

Fig. 9. Shear force vs. strain at equilibrium (fin-plate failure) for beam test with narrow end-posts.

#### 4.2. Test on beam with narrow end-post and notched flange

The beam with a 90 mm wide end-post and 90 × 60 mm notches to both flanges may be compared to the same test without notches. The mode of failure was expected to be in the region of the end-post close to the notch due to the concentration of compression stresses and the lack of restraint to buckling of the web.

The load-displacement curve for this test is shown in Fig. 10a and the behaviour was linear to a load of about 70% of the shear failure load of 279kN for the fin-plate connection side. Failure occurred by buckling of the narrow web at the notch (Fig. 11a). The ratio of the failure load of the notched fin-plate connection to the un-notched beam was 85%.

The test was continued as described in the protocol to a failure load of 298kN on the end-plate side (7% higher than the fin-plate side). The failure load was different in that buckling of the web at the notch was accompanied by significant lateral movement of the top flange relative to the end-plate (Fig. 11b). This suggests that the notched end-post is restrained more by the end-plate connection than the fin-plate, but the differences were relatively small. Failure occurred at a deflection of 18 mm, of which about 12 mm was due to plasticity.

The ratio of the failure load of the notched end-plate connection to the un-notched beam was 90%, which implies that the effect of the notch was less pronounced in this case.

The following observations were drawn:

- Fig. 10a shows that the end-plate connection is stiffer than the fin-plate connection but less so than the un-notched beam.
- Fig. 10c shows that for the end-plate connection, the transverse movement of the top flange occurs due to buckling of the narrow web at the notch that is seen in Fig. 11b.
- Figs. 12b and c show that the tensile strains in outside flanges are also small, indicating that the moments developed in the connections are also small.
- Fig. 13a shows that in the fin-plate connection, high plasticity occurs in the top notch which yields first (reaching its yield strain at ~175kN shear force, while the bottom notch reaches yield at ~225kN). Readings are in good agreement with the failure mode in Fig. 11a which shows the pronounced buckling of the narrow web at the top notch.
- Fig. 13b shows similar behaviour in the end-plate connection but with lower overall strains.

#### 4.3. Test on notched cellular beam with half infill plate

The beam with a half infill plate to the first cell satisfied the minimum width of end-post criterion but the infill plate was 10% thinner than the web of the beam so that the infill plate might lead to a reduced buckling load. Also, the weld of the infill plate to the web, although continuous, may not achieve full penetration which would reduce its

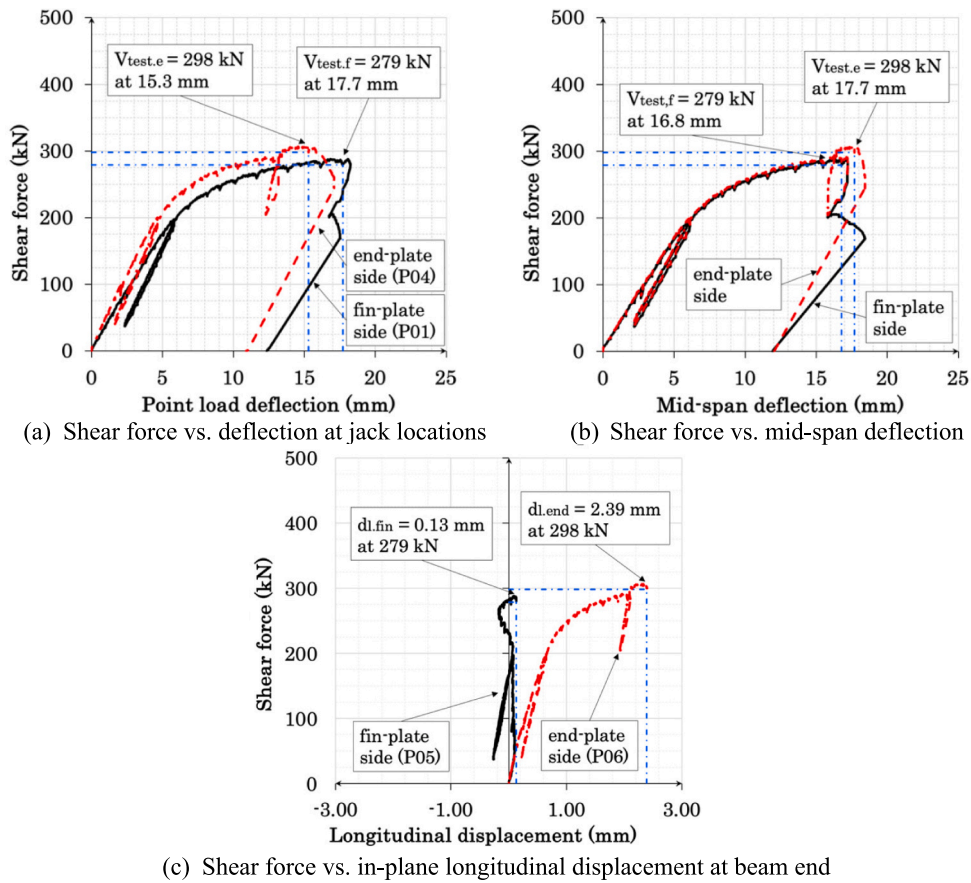


Fig. 10. Load-displacement curves for beam test with narrow end-posts and notches to flanges.

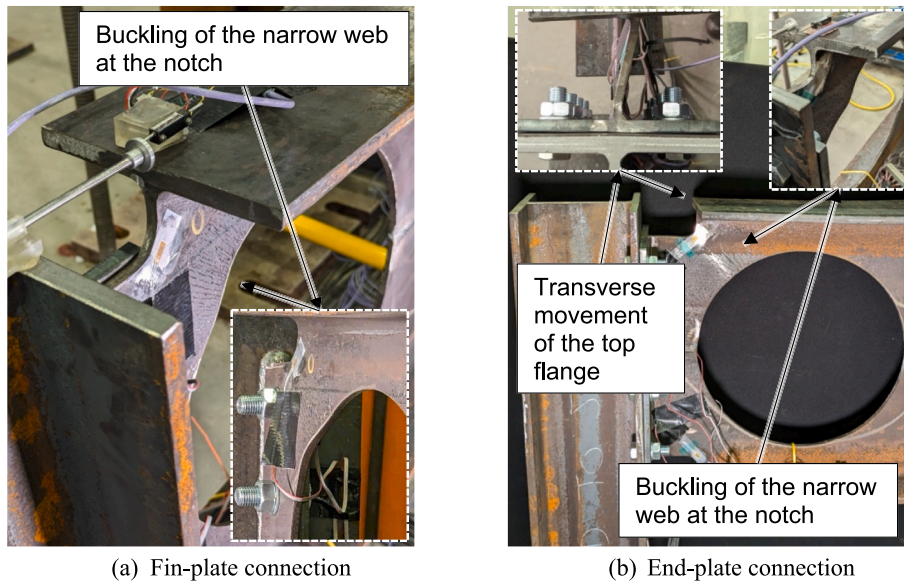


Fig. 11. Failure modes for beam test with narrow end-posts and notches to flanges.

local resistance to buckling.

The load-displacement curve for this test is shown in Fig. 14. The behaviour was linear until about 75% of the shear failure load of 398kN for the fin-plate connection side. Failure occurred by buckling of the half infill plate in compression (Fig. 15a) due to the shear force transferred to it from the top Tee. Visually, the weld of the infill plate to the web seemed to act as only partially fixed and buckling occurred over half of

the depth of the infill.

The test was continued as described in the protocol by reducing the shear force to 200kN and re-loading the jack on the end-plate side to a failure load of 417kN (5% higher than the fin-plate side). A similar mode of failure occurred at this side as shown in Fig. 15b. The failure load was taken after the load relaxation of the 'plateau' in the load-deflection curve at a deflection of about 18 mm, of which about 11 mm was due

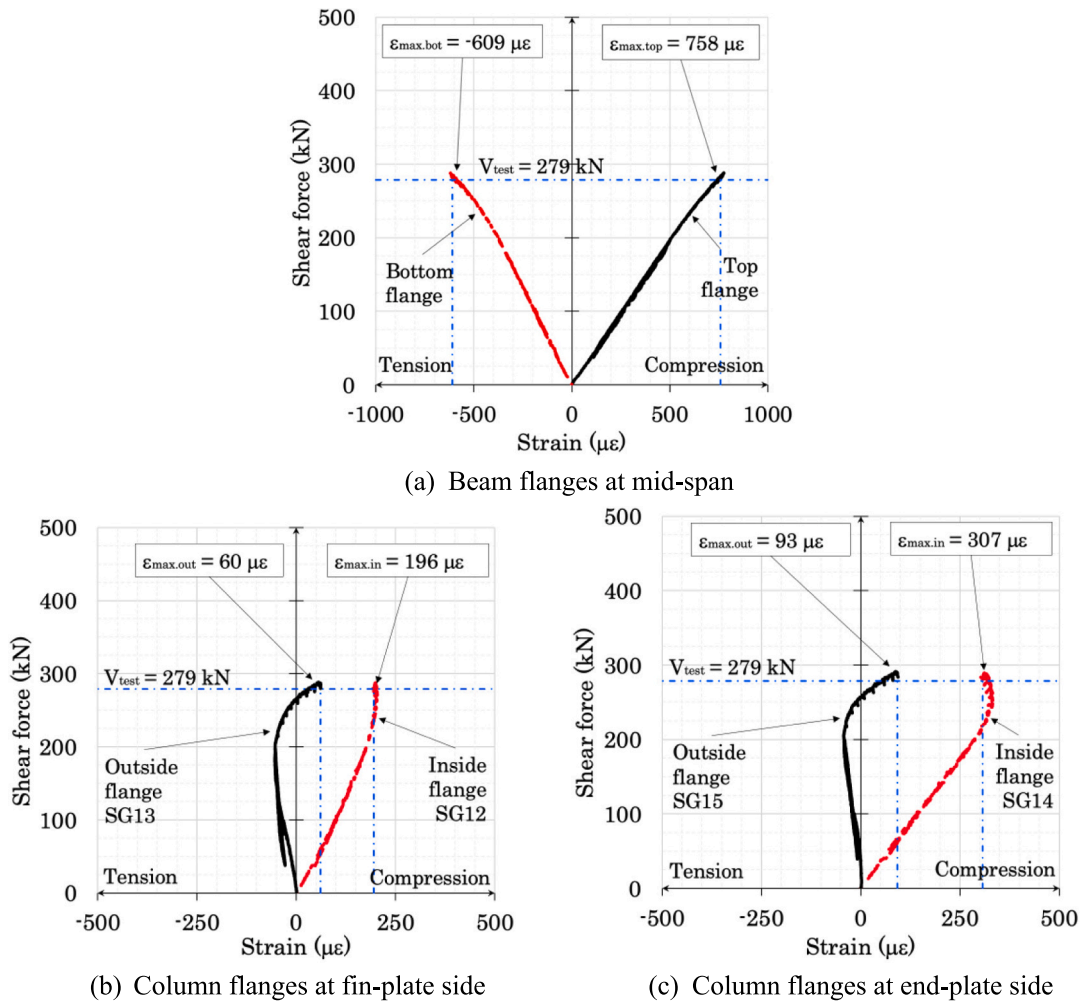


Fig. 12. Shear force vs. strain at equilibrium (fin-plate failure) for beam test with narrow end-posts and notches to flanges.

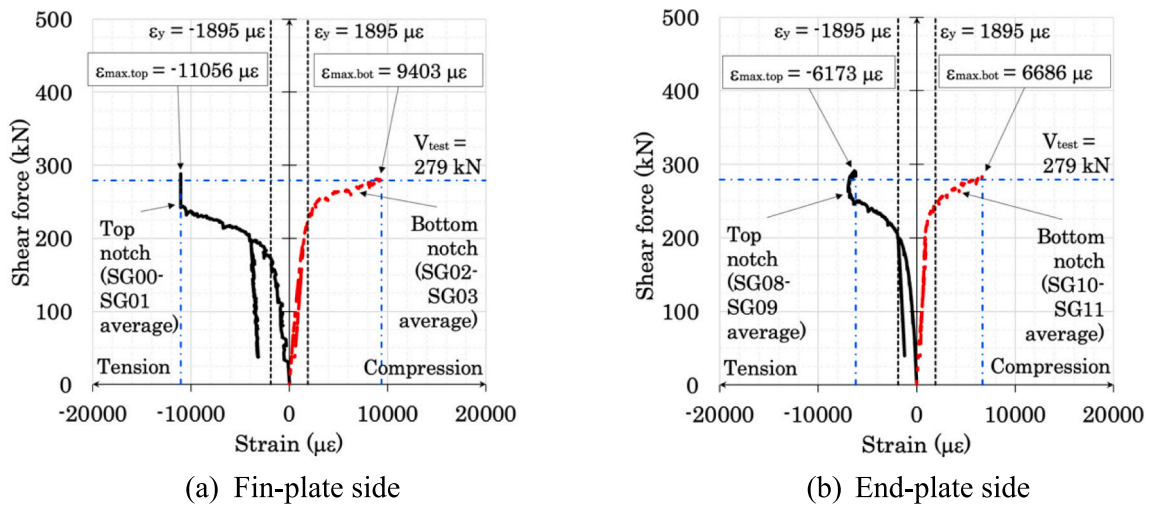


Fig. 13. Shear force vs. strain near notches for beam test with narrow end-posts and notches to flanges.

to plasticity.

The following observations were drawn:

- Fig. 14a shows that the end-plate connection is stiffer than the fin-plate connection, possibly due to the more pronounced effect of slip in the fin-plate connection in this test.
- Fig. 14c shows that the horizontal displacements are similar, in the range of 1–1.25 mm.

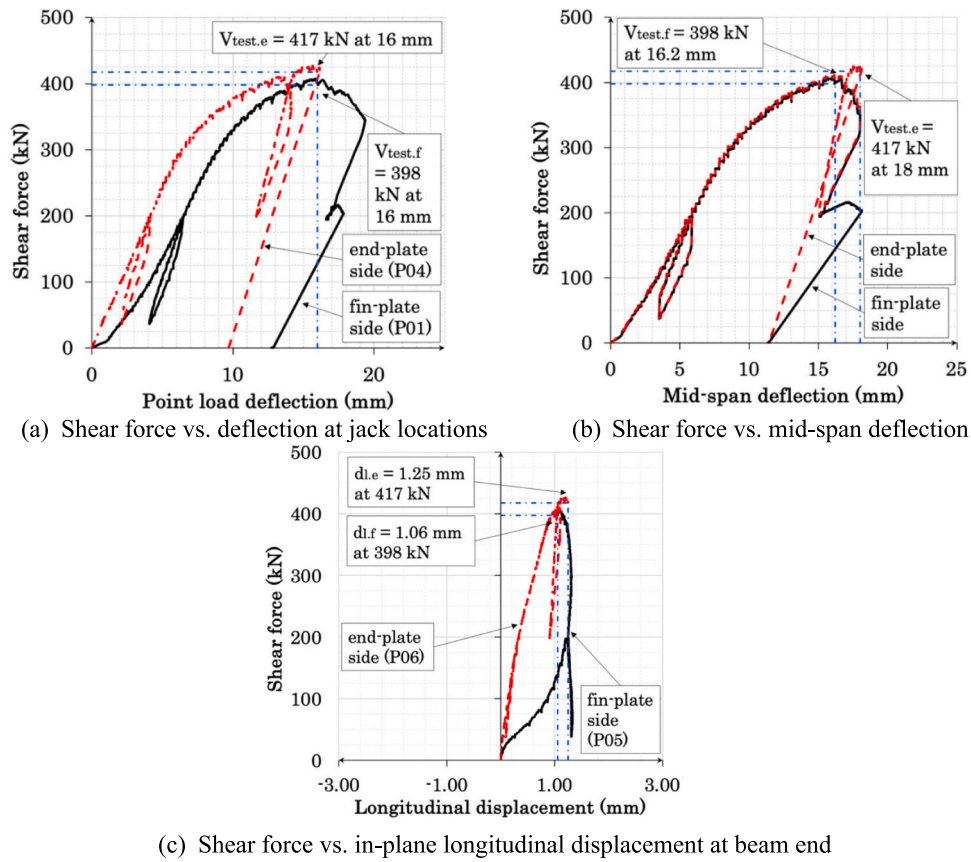


Fig. 14. Load-displacement curves for beam test with half infill plate and notches to flanges.

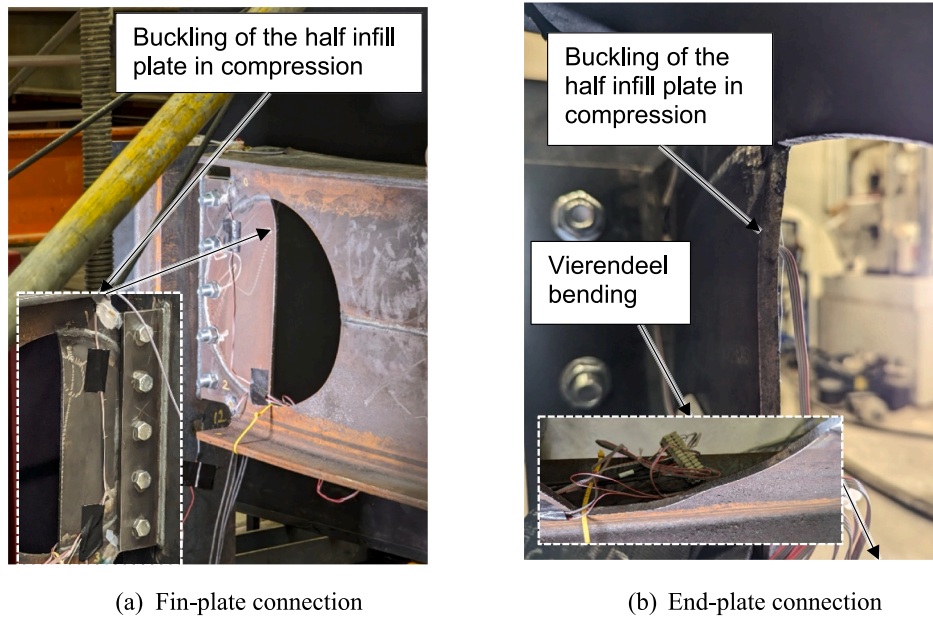


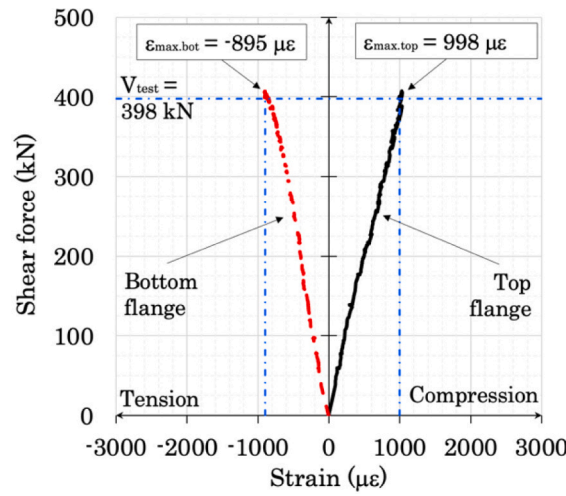
Fig. 15. Failure modes for beam test with half infill plate and notches to flanges.

- Figs. 16b and c show that compression strains are developed in the outside flange of the columns which indicates that sagging moments are developed in the connections.
- Figs. 17a and b show that low strains are reached in the top notch, whereas large plasticity occurs in the bottom notch. The end-plate strains in the bottom notch are twice as high as those on the fin-

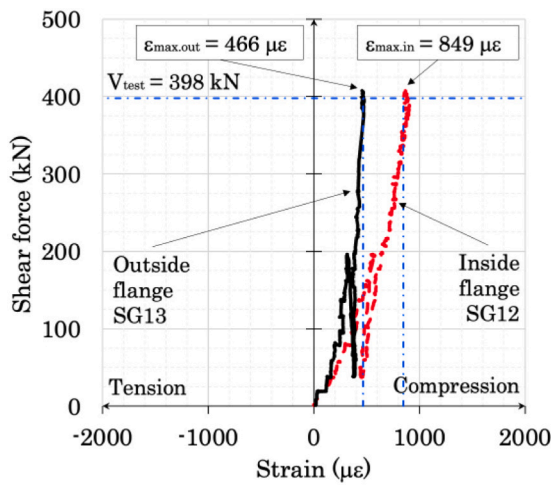
plate side. This suggests that high stress occurs due to redistribution of shear from the top Tee to the bottom Tee after buckling.

#### 4.4. Analysis of test failure loads

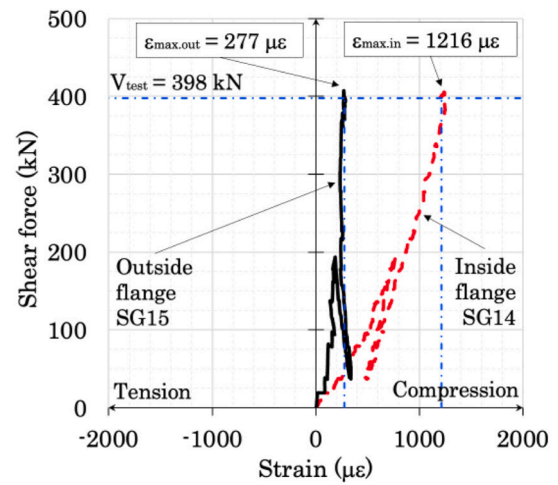
Table 2 presents the elastic section properties of cellular beam and



(a) Beam flanges at mid-span

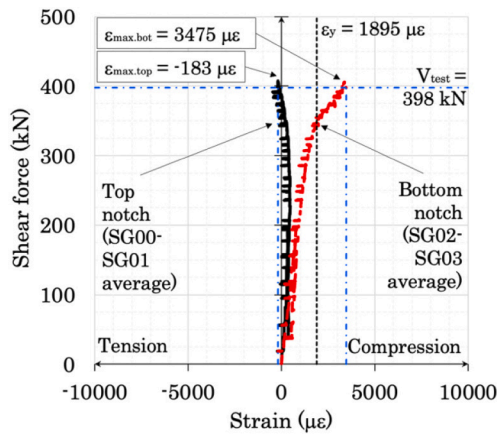


(b) Column flanges at fin-plate side

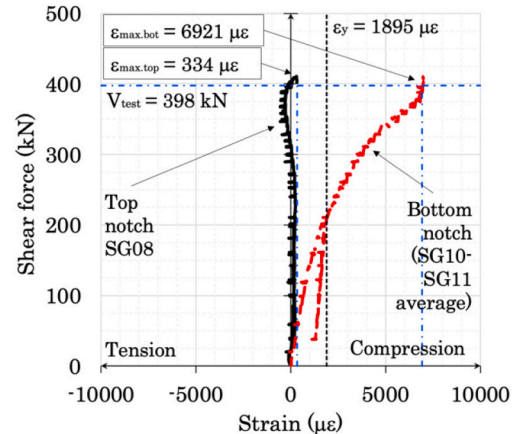


(c) Column flanges at end-plate side

Fig. 16. Shear force vs. strain at equilibrium (fin-plate failure) for beam test with half infill plate and notches to flanges.



(a) Fin-plate side



(b) End-plate side

Fig. 17. Shear force vs. strain near notches for beam test with half infill plate and notches to flanges.

columns. Table 3 summarises the bending moments in beam and at supports at fin-plate failure load obtained from the beam strains whereas Table 4 summarises the bending moments in columns and at supports at fin-plate failure load obtained from the column strains.

$$M_{test} = V_{test}(0.92 m - h_{col}) \quad (14)$$

$$M_{beam} = 0.5(\epsilon_{max,top} + \epsilon_{max,bot})E_{steel}Z_{el,y,beam,open} \quad (15)$$

**Table 2**

Elastic section properties of cellular beam and columns.

Element	Section	Area (mm <sup>2</sup> )	Inertia I <sub>yy</sub> (mm <sup>4</sup> )	Section modulus Z <sub>el</sub> (mm <sup>3</sup> )	Bending resistance M <sub>Rd</sub> (kNm)
Beam	Solid	9908	494 × 10 <sup>6</sup>	1760 × 10 <sup>3</sup>	700
CB 559x179x67	Opening	Area of Tee = 3154	446 × 10 <sup>6</sup>	1590 × 10 <sup>3</sup>	633
Columns UC 203x203x60	–	7640	61.2 × 10 <sup>6</sup>	584 × 10 <sup>3</sup>	344

**Table 3**

Bending moments in beam and at supports at fin-plate failure load obtained from the beam strains.

Test beam	M <sub>test</sub>	M <sub>beam</sub>	M <sub>conn. beam</sub>	V <sub>test</sub>	F <sub>Tee</sub>
Narrow end-post	265 kNm	241 kNm	24 kNm	325 kN	–4 kN
Narrow end-post with notches to flanges	227 kNm	228 kNm	–1 kNm	279 kN	99 kN
Half infill plate with notches to flanges	324 kNm	316 kNm	8 kNm	398 kN	68 kN

NOTE: M<sub>test</sub> is the applied moment at load position corresponding to the finplate failure load determined using eq. (14), M<sub>beam</sub> is the bending moment calculated from the stresses in the flanges at mid-span of the beam using eq. (15), M<sub>conn.beam</sub> is the bending moment transferred from the beam to its supports via the connections equal to M<sub>test</sub> – M<sub>beam</sub>, and F<sub>Tee</sub> is the axial force in bottom tee section calculated using eq. (16).

**Table 4**

Bending moments in columns and at supports at fin-plate failure load obtained from the column strains.

Test beam	Connection	M <sub>test</sub>	M <sub>conn</sub>	M <sub>col</sub>	% x M <sub>test</sub>
Narrow end-post	Fin-plate	265 kNm	0.7 kNm (hogging)	35 kNm	13%
	End-plate		22.7 kNm (hogging)	55 kNm	21%
Narrow end-post with notches to flanges	Fin-plate	227 kNm	–7.2 kNm (sagging)	22 kNm	10%
	End-plate		–11.1 kNm (sagging)	18 kNm	8%
Half infill plate with notches to flanges	Fin-plate	324 kNm	*–55.9 kNm (sagging)	–14.2 kNm	4%
	End-plate		–33.2 kNm (sagging)	8.5 kNm	3%

NOTE: M<sub>conn</sub> is the bending moment in the connection calculated from the strain in the outside flange of the column determined using eq. (17), M<sub>col</sub> is the bending moment in the column equal to M<sub>ecc</sub> + M<sub>col</sub>, M<sub>ecc</sub> is the bending moment due to eccentric shear force calculated as per expression (18).

\* The strain gauge reading could possibly be off, or the calculated value is overly conservative.

$$F_{Tee} = (\varepsilon_{max,top} - \varepsilon_{max,bot}) E_{steel} A_{Tee} \quad (16)$$

Where V<sub>test</sub> is the shear force at failure, h<sub>col</sub> is the depth of the column cross-section, ε<sub>max,top</sub> and ε<sub>max,bot</sub> are the maximum strain readings at mid-span of the beam recorded in the top and bottom flanges at failure, Z<sub>el,y,beam.open</sub> is the elastic section modulus of the beam at an opening, and A<sub>Tee</sub> is the area of a Tee as per Table 2.

$$M_{test} = \varepsilon_{max,out} E_{steel} b_{col} t_{col,fl} (h_{col} - t_{col,fl}) \quad (17)$$

$$M_{test} = V_{test} \frac{h_{col}}{2} \quad (18)$$

Where ε<sub>max,out</sub> is the maximum strain reading in the outside column flange at failure, b<sub>col</sub> is the width of the column cross-section, and t<sub>col,fl</sub> is the flange thickness of the column cross-section.

The comparison between the failure loads and calculated shear and bending resistances is presented in Table 5, while the analytical representation of the failure modes was shown in Fig. 18. For the tests with narrow end-posts, both *Vierendeel* bending and horizontal end-post shear may control, whereas for the tests with the half infill plate, vertical shear in the Tees was critical. The vertical shear force also led to buckling of the infill plate without evidence of shear failure of the Tees.

In all cases, the failure load of the end-post with an end-plate connection exceeded that of the fin-plate connection but the differences in the failure load were only 3 to 7% for the two connection types.

The test shear failure loads are presented in Table 6 in comparison to the prediction of the design formulae in EN 1993-1-13 using measured material strengths and dimensions. It can be seen that the ratio of the failure load to the design prediction using measured steel thicknesses and strengths was in the range of 1.64 to 1.82 for the case of the 4 tests with narrow end-posts, which may be considered to be overly conservative, and some improvements may be made whilst still maintaining an acceptable level of safety. For the test with half infill plates, the ratio of the failure load to the design prediction was of 1.35 and 1.51 for the 2 connection types which is less conservative.

## 5. Concluding remarks

Cellular beams of 560 mm depth with 400 mm diameter circular web openings and with bolted fin-plate and end-plate connections were tested to failure to determine the shear resistance of the end-posts between the outer openings and their connections. The tests showed that:

- The beam with 90 mm wide end-posts failed at a shear force of 325kN on the fin-plate side and 331kN (+2%) on the end-plate side. The mode of failure was by horizontal shear and in-plane bending of the narrow end-post on the fin-plate side and by *Vierendeel* bending on the end-plate side, showing that the end-plate increased the resistance of the narrow end-post in horizontal shear and bending.
- The beam with the same 90 mm wide end-post and with a 90 mm wide x 60 mm deep notches cut in the flanges failed at a shear force of 279kN on the fin-plate side and 298kN (+7%) on the end-plate side. This showed that the notches reduced the shear resistance of the narrow end-posts by 10 to 14%. The mode of failure was by buckling of the reduced web at the notch accompanied by lateral movement of the flange at the notch on the end-plate side.
- The same notched beam with a half-infill plate of similar thickness to the beam web failed at a shear force of 398kN on the fin-plate side and 417kN (+5%) on the end-plate side. This showed that the half-infill plate increased the failure load by 40 to 43% compared to the test without infill plates. The mode of failure was by buckling of the infill plate on both sides accompanied by *Vierendeel* bending at the half opening at the higher shear force on the end-plate side.

The test failure loads were compared to the end-post buckling resistances given in the draft EN 1993-1-13 exceeded the predicted resistances by 35 to 83% using measured material strengths. However, EN 1993-1-13 does not present a definitive design method for the end-posts with half infill plates or for notched beams. In all cases, the shear failure loads exceeded the factored design shear force of 200kN that would be expected of this cellular beam section and its realistic design span.

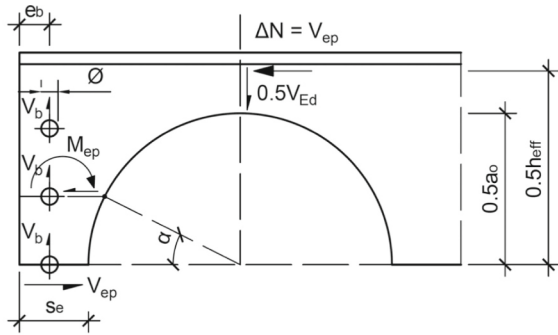
## CRedit authorship contribution statement

Konstantinos Daniel Tsavdaridis: Writing – review & editing,

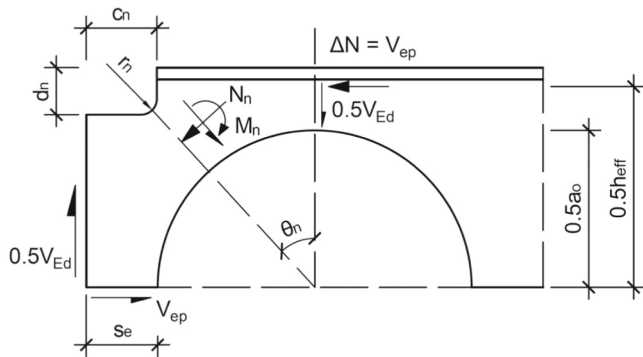
**Table 5**  
Summary of failure modes and predicted resistances.

Beam	Connection	Shear failure load	$V_{test}/V_{Rd}$	$V_{test}/V_{Vier,Rd}$	$V_{test}/V_{ep,Rd}$	$M_{test}/M_{Rd}$	Mode of failure in test
Narrow end-post	Fin-plate	325 kN	0.88	–	<b>0.96</b>	0.40	Horizontal shear and bending in end-post
	End-plate	331 kN	0.90	<b>1.09</b>	0.98	0.40	Vierendeel bending of first opening
Narrow end-post with notch	Fin-plate	279 kN	0.76	–	0.82	0.34	Local buckling of narrow web at notch
	End-plate	298 kN	0.81	0.99	0.88	0.36	Horizontal flange movement and local buckling at notch
Half infill plate with notch	Fin-plate	398 kN	<b>1.08</b>	–	0.70	0.48	Buckling at the top of half infill plate
	End-plate	417 kN	<b>1.13</b>	1.95	0.73	0.51	Buckling at half infill plate and Vierendeel bending

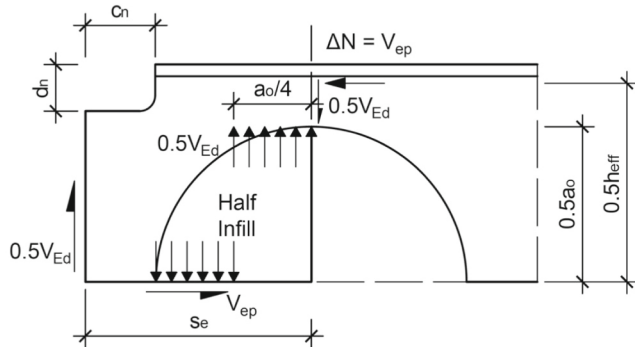
NOTE:  $V_{Rd}$  is the vertical shear resistance at centre-line of opening,  $V_{Vier,Rd}$  is the shear resistance in Vierendeel bending at the first opening,  $V_{ep,Rd}$  is the vertical shear resistance due to horizontal shear failure of the end-post,  $V_{test}$  is the shear force at failure,  $M_{Rd}$  is the bending resistance of the beam at the centre-line of the opening, and  $M_{test}$  is the applied moment at load position determined using eq. (14).



(a) End-post shear and bending in narrow end-post



(b) Compression and bending at notch in narrow end-post



(c) Buckling of half infill plate in compression

**Fig. 18.** Modes of failure of end-posts in the tests.

Supervision, Project administration, Methodology, Funding acquisition, Data curation, Conceptualization. **Brett McKinley:** Methodology, Investigation, Data curation. **Dan-Adrian Corfar:** Writing – original draft, Visualization, Software, Formal analysis, Data curation. **R. Mark Lawson:** Writing – review & editing, Validation, Supervision,

**Table 6**  
Summary of failure modes, shear failure loads and comparison with the prediction to EN 1993-1-13 using measured properties.

Test beam	Connection type	Shear failure load	EN1993-1-13 prediction
Narrow end-post (90 mm wide)	Fin-plate	325 kN	178 kN
	Full depth end-plate	331 kN (+2%)	188 kN
Narrow (90 mm wide) end-post with 90x60mm notches to flanges	Fin-plate	279 kN	171 kN
	Partial depth end-plate	298 kN (+7%)	178 kN
Half infill plate (200 mm wide) with 90x60mm notches to flanges	Fin-plate	398 kN	264 kN
	Partial depth end-plate	417 kN (+5%)	309 kN

Resources, Formal analysis, Conceptualization.

**Declaration of competing interest**

The authors declare that they have no known competing financial interests or personal relationships that could have appeared to influence the work reported in this paper.

**Data availability**

No data was used for the research described in the article.

**Acknowledgements**

The tests were performed in the Heavy Structures Laboratory at City, University of London and the test work was sponsored by Westok | Kloeckner Metals UK, who also fabricated the test beams, columns and their connections. The work was carried out to assist in the preparation of EN 1993-1-13 Eurocode 3.

**References**

- [1] F. Almutairi, K.D. Tsavdaridis, A.A. Rodríguez, I. Hajirasouliha, Experimental investigation on demountable steel-concrete composite reduced web section (RWS) connections under cyclic loads, Bull. Earthq. Eng. (2023).
- [2] American Institute of Steel Construction Design Guide 31, Castellated and Cellular Beam Design, 2016.
- [3] British Standards Institution, BS EN 1993-1-1: Design of Steel Structures: Part 1.1 General Rules and Rules for Buildings, (replaces 2005 version), 2022.
- [4] CEN European Committee for Standardisation: EN 1993-1-13, Part 1-13: Rules for beams with large web openings. CEN/TC250/SC3: Draft for approval, October 2022.
- [5] L.F. Grilo, R.H. Fakury, A.K. Reis de Castro e Silva, G. de Souza Verissimo, Design procedure for the web-post buckling of steel cellular beams, J. Constr. Steel Res. 148 (2018) 525–541.
- [6] R.M. Lawson, S.J. Hicks, The Design of Composite Beams with Large Web Openings, SCI P355., The Steel Construction Institute, 2011.
- [7] B. Li, Q. Yang, N. Yang, An investigation on aseismic connection with opening in beam web in steel moment frames, Adv. Struct. Eng. 14 (3) (2011) 575–587.

- [8] H. Nazaralizadeh, H. Ronagh, P. Memarzadeh, F. Behnamfar, Cyclic performance of bolted end-plate RWS connection with vertical-slits, *J. Constr. Steel Res.* 173 (2020) 106236.
- [9] P. Panedpajaman, T. Thepchatri, S. Limkatanyu, Novel design equations for shear strength of local web-post buckling in cellular beams, *Thin-Walled Struct.* 76 (2014) 92–104.
- [10] R.G. Redwood, *Design of Beams with Web Holes*, Canadian Steel Industries Construction Council, 1973.
- [11] M.A. Shaheen, K.D. Tsavdaridis, S. Yamada, Comprehensive FE study of the hysteretic behaviour of steel-concrete composite and non-composite RWS beam-to-column connections, *J. Struct. Eng. ASCE* 144 (9) (2018).
- [12] The Steel Construction Institute, *Joints in steel construction: simple joints to Eurocode 3*, SCI P358 (2011).
- [13] K.D. Tsavdaridis, C.K. Lau, A.A. Rodríguez, Experimental behaviour of non-seismical RWS connections with perforated beams under cyclic actions, *J. Constr. Steel Res.* 183 (2021).
- [14] K.D. Tsavdaridis, C. D’Mello, Web buckling study of the behaviour and strength of perforated steel beams with different novel web opening shapes, *J. Constr. Steel Res.* 67 (10) (2011) 1605–1620.
- [15] K.D. Tsavdaridis, F. Faghiih, N. Nikitas, Assessment of perforated steel beam-to-column connections subjected to cyclic loading, *J. Earthq. Eng.* 18 (8) (2014) 1302–1325.
- [16] K.D. Tsavdaridis, T. Papadopoulos, A FE parametric study of RWS beam-to-column bolted connections with cellular beams, *J. Constr. Steel Res.* 116 (2016) 92–113.